PROCEEDINGS, 47th Workshop on Geothermal Reservoir Engineering
Stanford University, Stanford, California, February 7-9, 2022
SGP-TR-223

High Resistivity Well Cement for Underground Wells Suitable for Sealing Monitoring Equipment

Lance Sollohub[1], Timothy Johnson[2], Toshifumi Sugama[3], Tatiana Pyatina[3]

[1]Cudd Energy Services

[2]Pacific North National Laboratory

[3]Brookhaven National Laboratory

734 Brookhaven Ave. Upton, NY 11973

tpyatina@bnl.gov

Keywords: geothermal well cement, electrically resistive cement, enhanced geothermal wells

ABSTRACT

This paper presents cement design and evaluations for application in underground wells with monitoring equipment. Cement was needed to secure the suite of instruments in the nearly horizontal monitoring holes and to seal them preventing the movement of fluids along the length of the wells. Design criteria included an electrically resistive cement, with the resistivity of no less than 1000 Ohm-m, and cement heat of hydration temperature not exceeding the temperatures allowed by the installed instruments and their cables insulation, set to be below 75°C. Additionally, cement was to have low rheological parameters to easily flow into tight spaces between the cables and the equipment (on the order of 5 mm) while still being stable and able to provide a tight seal against the cable insulation and a PVC pipe (no shrinkage). The paper discusses cement laboratory design and evaluations showing effect of various additives on cement resistivity, compressive strength, toughness, shear bond strength with Teflon coated wire. Electrical resistivity of above 2,000 Ohm-m was achieved. Optimization of the final field applicable formulations, following American Petroleum Institute (API) procedures showed that designs needed further modifications likely due to the significant variations in the performance of granulated blast furnace slag intended for the job execution and slag tested in the early laboratory tests.

1. INTRODUCTION

In early 2017, the Department of Energy's Geothermal Technologies Office funded National Laboratories to focus on transformational enhanced geothermal systems (EGS), to establish a collaborative experimental and model comparison initiative - the EGS Collab. The EGS Collab is a small-scale field site where the subsurface modeling is validated against controlled, small-scale, in-situ experiments focused on rock fracture behavior and permeability enhancement. Cement was needed to secure the suite of instruments in the nearly horizontal monitoring holes and to seal them preventing the movement of fluids along the length of the wells. To achieve desirable rheological, mechanical, and setting properties cement formulations are usually modified with various existing additives. However, one of the requirements for the monitoring well cements was low electrical conductivity or high electrical resistivity of above 1,000 Ohm-m, which is not a property that can be easily achieved with cementing additives that are commonly ionic compounds.

There is little information in literature on design and application of underground cementitious materials with high resistivity. The main focus of reported electrical conductivity in cements is the early-stage cement pastes conductivity as a predictor of the cement hydration and strength development[1]. Lately significant volume of published articles reported conductivity enhancement with carbon-based materials[2–4]. However, addition of styrene-butadiene latex to carbon fibers reinforced cement was shown to increase its resistivity[5]. Another use of conductivity measurements is its connection with the cement permeability related to ions transport through cement layer, which is of interest to predict cement's susceptibility to chlorine-caused corrosion, acid corrosion, and metal protection by cement from corrosion[6]. Since water plays the major role in most degradation mechanisms of cement through reactions with non-hydrated cement particles and by providing transport of harmful species, the electrical properties can be used to predict durability of cement-based materials. It was shown that increased of ions content and water amount as a continuous media for ions transport reduce cement resistivity. Recently self-sensing cements with properties of high electrical conductivity have been intensively studied[7].

A few studies looked at the effect of blend components and cementing additives on cement's electrical properties. Effect of cement blend components on the set cement conductivity was reported for fly ash, silica, fume, and ground granulated blast furnace slag[8]. All three components increased early resistivity of cement. Silica fume and especially slag were shown to accelerate development of electrical resistivity in a work where high resistivity cement was designed to prevent stray current from direct-current light rail systems that can corrode underground metal pipes, potentially causing significant damage to utility lines[9].

Some earlier research reported effect of additives on the early-stage cement conductivity[10]. A study of electrical conductivity of cement pastes made with OPC, OPC clinker and various additives showed that after the slurry mixing the conductivity increased but then decreased steadily with a short interruption by a transient maximum. All the tested set accelerators and retarders increased the conductivity of the cement. However, gypsum was shown to decrease the transient maximum when added at a certain concentration.

The goal of this work was to design cement formulation with a combination of properties that included low rheological parameters (very fluid slurries), timely mechanical properties development, stability, and high electrical resistivity for nearly horizontal monitoring wells in the frame of EGS Collab.

2. MATERIALS AND METHODS

2.1 Electrical Resistivity Measurements

A modified ASTM C1760 method was used to measure electrical resistivity of cement samples. For all the measurements control cement that was used in the first round of monitoring wells was also prepared and its conductivity was compared with the cement modified with the additives. The samples were subjected to a constant voltage (to mitigate induced polarization) and the current was measured one minute later. To ensure contact between the samples and the probes, filter paper wetted with 0.1M potassium chloride solution was placed between the sample and the probe. The resistivity was calculated from the following expression: $\rho=V/I\times A/L\times 106$, where ρ is resistivity in Ohm·m, V is potential in V (10V), I is current in µA, A is a cross section of a cylindrical sample in m, and L is the sample's length in m.

To eliminate contribution of the contact resistivity additional measurements were done on selected samples using DC-circuit with two resistors in series, the reference resistor, and the grout sample. The grout sample was connected to the circuit using metallic current electrodes. The potential electrodes were metal posts that came into contact with the sample. They were separated by 1/3 of the sample length distance, while been centered on the sample. In this set up a measurement is taken by applying a source voltage and measuring the reference and sample voltages. To avoid electrode polarization the voltage source is applied as an alternating square wave or sine wave. The sample resistivity (rho) is computed as follows: rho = Rsamp*(A/L), where A is the cross-section area of the sample and L is its length, Rsamp = Vsamp/Ic, and Ic=Vref/Rref (Vref and Rref – are reference electrode voltage and resistance respectively).

2.2 Samples Preparation and Testing – laboratory design optimization

Two types of Ordinary Portland Cement (OPC) were used in this work: OPC type I/II (provided by Trabits group) and OPC, class A (provided by Cudd Energy Services). Fly Ash, type F (FAF) was also obtained from Cudd Energy Services. The XRD analysis of FAF showed that it included three major crystalline products: mullite ($3Al_2O_3.2SiO2$), silica (SiO_2), and hematite (Fe_2O_3). Granulated blast furnace slag (GBFS) and pumice were essentially amorphous. The composition of the blend components is given in Table 1. A self-cross-linking acrylic copolymer, Hycar® 26-0688 emulsion was obtained from Lubrizol Advanced Materials. Purified lignosulfonate dispersant was supplied by Schlumberger Inc. VinnaPass vinyl acetate-based polymer was obtained from Wacker, the acrylic epoxy hybrid Maincote™ AEH-10 was supplied by Dow Inc. All the cement additives, including dispersant, gypsum, styrene-butadiene latex, anti-foaming agent, were provided by Cudd Energy Services. EDTA was obtained from Sigma Aldrich, Cement formulation used in the first round of monitoring wells was prepared using OPC class I/II (10 wt.%), pumice (from Hess pumice products) (40 wt.%) GBFS (from Lafarge North America Inc.) (50 wt.%). The blend was dry-mixed before adding water (water-to-cement ratio 0.5); the slurry was hand-mixed until getting a uniform suspension for about 2 minutes. The slurries were poured into 20 x 40 mm cylindrical molds, covered with aluminum foil, and left to cure at room temperature. The cement bonding to the Teflon insulation of the instrumental wires was tested in "pull out" tests. In these tests plastic tubes with 10 mm diameter were filled with cement slurry and the wire was inserted in the middle of the tube. The tube opening was covered with aluminum foil and left to cure at room temperature until mechanical testing. To evaluate slurry flowability, slump was measured by using a polyethylene cone with the top hole of 20 mm diam., bottom hole of 45 mm diam., and 40 mm height. The cone was placed on a flat carbon steel plate, filled with cement slurry, and slowly lifted, allowing the slurry to spread. The slurry slump was measured 20s later. The unconfined sheath samples surrounding carbon steel or formation tube were prepared in the following manner. The disk-shaped wooden tube-holder (49-mm diam. by 13-mm-high) with a center hole (26- mm-diam.) was placed at the bottom of the cylindrical paper-mold with 48-mm-inner diam. and 100-mm length. The tube (125-mm-long x 25-mm-outer diam. x 3-mm-wall thickness) was inserted into the center hole of the wooden casing holder located at the bottom of the mold. The hand-mixed slurry was poured in an annular space between tube and the mold to prepare a sheath sample 23 mm thick and 74 mm high.

Electromechanical Instron System Model 5967 was used to obtain all mechanical properties. XRD (40 kV, 40 mA copper anode X-ray tube) was used for samples characterizations. The results of XRD tests were analyzed using PDF-4/Minerals 2021 database of International Center for Diffraction Data (ICDD). Additionally, JEOL 7600F Scanning Electron Microscope (SEM) image analyses coupled with EDX elemental composition survey were done for the typical spots on freshly broken samples. Cement samples were coated with silver to decrease the charging effects prior to the analyses.

Table 1: composition of starting materials.

Component	Oxide composition, wt.%								
	Al_2O_3	CaO	SiO_2	Fe_2O_3	Na_2O	K_2O	TiO_2	MgO	SO_3
OPC type I/II	5.2	65	20.3	3.2	0.20	1.0	-	2.6	2.5
OPC, class A	8.2	57	18.3	3.2	-	4.8	-	0.98	7.5
GBFS	12.9	38.6	35.3	1.1	-	-	0.40	10.7	1.0
FAF	35	2.7	50	7.1	0.30	3.1	1.6	-	-
Pumice	13.5	0.80	76	1.1	1.6	1.8	0.2	0.05	-

For the final field design and slurry optimization tests were performed following American Petroleum Institute (API) testing procedure 10B.

3. RESULTS AND DISCUSSION

3.1 Requirements and Constrains for Cement Design

The optimized cement was to meet several requirements that included sealing the wells and the monitoring equipment, providing high electrical resistivity of no less than 1000 Ohm-m, possessing low temperature of hydration with the limit being below 75°C, high fluidity (low rheological parameters) to secure tight spaces between the cables of the equipment, while being very stable for applications in nearly horizontal holes. The cement was also to provide a tight seal against the cable insulation, including Teflon and a PVC pipe (no shrinkage). For the optimal performance of the monitoring equipment, cement foaming was not allowed.

The two common ways to achieve desirable cement performance are formulation of a cementitious blend with specific properties and blend properties adjustment by introduction of functional additives. There exist a wide range of OPC additives. Table 2 shows necessary formulation ingredients for achieving target slurry and cement properties as well as their side effects.

It can be seen from the table that required combination of properties is not easy to achieve because of the significant secondary (undesirable effects) of cement modifying additives and blend components. Most of the cement additives are salts that produce ions in cement slurries significantly increasing slurries electrical conductivity, which is not acceptable for the current material requirements. This is true for dispersants that allow decrease of rheological parameters for good slurry penetration into tight spaces, anti-settling additives helping with the slurry stability, and accelerators that help fast set and development of mechanical properties under low temperatures. The requirements of low heat of hydration and high electrical resistivity limit the amount of cement in the blend since its hydration is strongly exothermic and the ions released during the hydration increase cement conductivity. Low cement content in a blend negatively affects the mechanical properties that cement develops. The table clearly shows that achieving one property can easily compromise other desirable characteristics of the target material.

Table 2: Cementitious compositions and additives providing target properties and their secondary effects.

Target property	Formulation composition and additives	Secondary effect on slurry and cement properties
Good flowability, low rheological parameters (filling tight spaces)	Dispersant, increased water content	Decreased electrical resistivity, delayed setting (retardation) at low temperatures, delayed development of mechanical properties
Slurry stability (horizontal well)	Dispersant, anti-settling additives, silica fume	As above for dispersant, increased rheological parameters with anti-settling additives and silica fume
Mechanical properties (fast development to avoid possible slurry losses and slurry instability)	Sufficiently high cement content in blends, accelerator	Decreased electrical resistivity, increased heat of hydration
Non-shrinking, good bonding (wires' insulation, PVC)	Gypsum (expansion), latex (bonding), fibers	Possibly compromised mechanical properties from matrix damage at too high expansion, delayed set and development of mechanical properties at low temperatures, increased foaming, increased rheological parameters (gel strength)
High electrical resistivity	Blends including slag, silica fume, fly ash, pumice, low cement content	High rheological parameters, low fluidity, inconsistent performance of secondary cementitious materials (slag, fly ash). Low cement content may result in poor mechanical properties.
Toughness for good combination of strength and ductility during fracturing experiments.	Polymers, fibers	Increased foaming, possibly delayed set, and development of mechanical properties at low temperatures, in the case of fibers increased rheological parameters.
Low heat of hydration	Low cement content, blends of cement with supplementary materials (fly ash, silica fume, pumice)	Poor mechanical properties
No foaming	Antifoam	Unknown effect on electrical resistivity

3.2 Formulation Optimized for Rheological, Mechanical, and Setting properties

The original cement blend was GBFS (slag) at 50%, pumice at 40%, and Portland type I/II at 10% (all by weight); the water/cement ratio was 0.50. This blend demonstrated acceptable resistivity of about 2000 Ohm-m after a month of curing but was difficult to mix (the amount of water had to be increased on the spot despite preliminary laboratory evaluations) and the cement seal was broken with water leaking out of the wells after the stimulation experiment. The original blend properties were evaluated in the flow and mechanical performance tests. Table 3 and Figure 1 (left) show the results.

Table 3: Mechanical properties of the original blend (50% slag, 10% OPC type I/II, 40% pumice).

Curing time, days	Compressive strength, psi	Young's modulus, psi	Toughness, Nmm/mm^3	Sheath-shear bond strength casing	Sheath-shear bond strength formation	"Pull out" rapture bond strength, psi
7	460 ± 30	-	0.11 ± 0.002	-	-	~145
30	920 ± 60	75,000 ± 37,000	0.11 ± 0.01	150 ± 20	120 ± 60	-

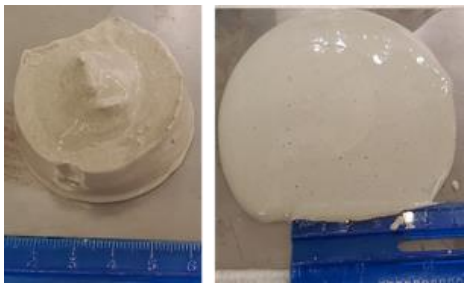

Figure 1: Spread of a given volume of the original slurry design with water-to-blend ratio 0.5 (left) and latex-modified slurry with water-to-blend ratio 0.42 (right)

The mechanical properties of the blend after 30 days of hydration can be considered as final. These values are typical for a low-temperature OPC slurry with secondary materials. However, the cone test of the slurry clearly showed its low fluidity. To increase slurry fluidity without increasing its water content that would result in increased conductivity, dispersants are added. For low-temperatures lignosulfonate (LS) dispersants are commonly used in oil field cement designs. To improve cement toughness polymers can be used. The original formulation was modified with the LS dispersant and tested with the addition of 2 different polymers that are known to have a positive effect on mechanical properties of the slurries and their rheological parameters: latex and acrylic polymer emulsion, Hycar. Mechanical properties of the modified slurries after 7 days (or 14 days) of hydration are shown in Table 4 and the cone test for the slurry with 2 gal/sk latex in Figure 1 (right). Both LS dispersant and latex dramatically increased fluidity of the slurry. In fact, the latex allowed better fluidity with lower water content than that in the original design, as can be seen in Figure 1. Replacement of OPC type I/II with class G OPC noticeably increased early strength development (1400 psi vs 720 psi for the similar design with type I/II) and, as a result, increased the set cement toughness (0.4 vs. 0.13 Nmm/mm^3). The toughness increased further with the addition of the polymers (doubled for 2 gal/sk latex to 0.8 Nmm/m^3 and increased more than 8 times with 30% bwob Hycar polymer). The latex concentrations below 2 gal/sk did not produce any significant toughness increase (designs #7 and 8). The toughness increase with the addition of the polymers is illustrated in Figure 2. (Note the difference in the strain scale for the top and the bottom figures.) The area under the curve for the sample with latex (blue curve) is noticeably larger than for other designs. This corresponds to significantly higher sample ductility. Because of the very high cement ductility, instead of breaking into pieces, the sample compresses under the stress. This is even more true for the sample with 30% bwob Hycar polymer. The sample never breaks but yields to the pressure showing a very large strain extension (bottom graph Figure 2).

Table 4: Mechanical properties of the original blend modified with LS dispersant or polymer additives after 7 days of hydration.

#	Formulation	Curing time, days	Compressive strength, psi	Toughness, Nmm/mm^3	"Pull out" rapture bond strength, psi
1	Control: Slag/OPC I/II/Pumice	7	460 ± 30	0.11 ± 0.002	~145
2	Slag/OPC I/II/FAF	7	720 ± 400	0.13 ± 0.05	~116
3	Slag/OPC, class G/FAF	7	1400 ± 490	0.4 ± 0.004	-
4	Design #3 with LS dispersant (0.25% by weight of blend – "bwob")	7	1200 ± 24	0.31 ± 0.01	~130
5	Design #3 with 2 gal/sk latex	7	1500 ± 250	0.8 ± 0.2	~145
6	Design #4 with 2 gal/sk latex	14*	2400	0.9	~145
7	Design #3 with 0.1% bwob LS and 1 gal/sk latex	7	1140	0.45 ± 0.04	~130
8	Design #3 with 0.1% bwob LS and 1.5 gal/sk latex	7	820 ± 180	0.4 ± 0.18	~116
9	Design #2 with 30% bwob Hycar	14*	2900	3.3	~87
10	Design #2 with 15% bwob Hycar	7	740 ± 80	0.26 ± 0.04	-

* The slurry was not set after 7 days of curing

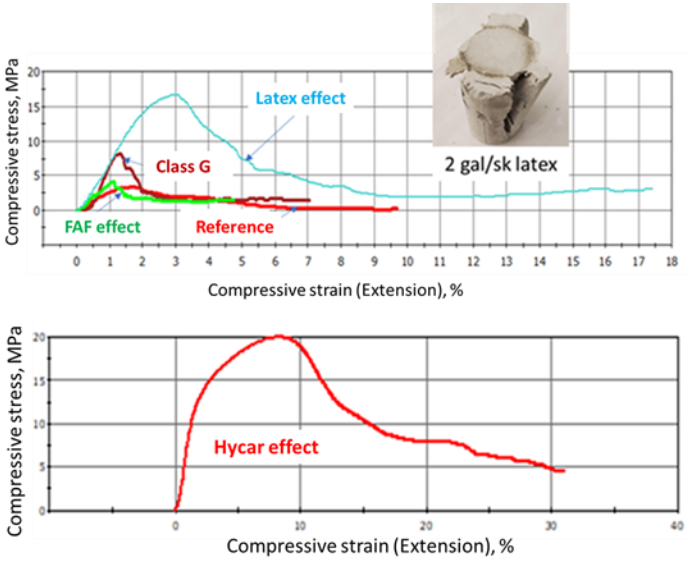

Figure 2: Stress-strain curves for some designs from Table 4 (#1 – reference, #2 – FAF effect, #3 – class G effect, #5 – Latex effect, and #9 – Hycar effect) and a photograph of Design #5 with 2 gal/sk latex after the compression tests.

However, the two clear concerns that arise with the addition of the dispersant and the polymers are delayed slurry set and decreased rapture bond strength. The drawback of the strongly delayed slurry set is a higher chance of slurry instability with possible segregation, precipitation and free fluid formation, and slurry loss to the formation. The data show that the combination of latex and dispersant strongly delays the slurry set suggesting synergetic retarding effect of these additives. As a result, the slurries with high dispersant content and latex were either not set after a week of hydration or their strength was low.

The decreased rapture bond strength is likely a result of slurry shrinkage in the presence of high polymer concentrations. Both the original design and the slurry with 30% bwob Hycar polymer cracked in the tubes used for the rapture bond tests. In the case of the Hycar-modified design this was the result of polymer-caused shrinkage.

These data illustrate the multifunctional nature of the additives that causes changes in slurry and set cement properties in more than one way, as explained in Table 1. Since addition of latex at 2 gal/sk improved both slurry fluidity and mechanical properties, including cement toughness, it was included into the first design of Cudd Energy Services.

Cudd Energy optimized cement slurry (Cudd cement) with very low rheological parameters for good flowability in tight spaces of the wells was a blend of class A cement and FAF (59/41 % by weight). It included silica fume (10 % bwob) for slurry stability, low heat of hydration, and electrical resistivity, gypsum (5% bwob) to prevent slurry shrinkage and to improve interface properties through controlled slurry expansion, cement set accelerator (3% bwob) for fast development of mechanical properties and prevention of slurry losses, and latex (3 gal/sk) for improved cement toughness.

The Cudd cement showed nearly 3-times higher bond strength with the metal (used as a proxy for PVC - cement bonding) and more than 4 times higher bond strength with the formation. The sheath sample of this cement stayed attached to the metal tube during the bond-strength tests while the original slurry just slid of the tube (Figure 3). The slurry was very fluid and easily filled a small tube with Teflon covered wire for rapture bond strength tests. Figure 3 shows both Cudd cement and control design, poor fluidity of which, resulted in voids in the tube (see the photographs before pull-out tests). The integrity of the Cudd cement persisted through the pull-out tests while control cement crumbled at one of the voids.

Table 5: Bond strength test results for the original blend and optimized Cudd cement formulation

Formulation	Cement-metal sheath shear bond strength, psi	Cement-formation sheath shear bond strength, psi	Rapture bond strength with Teflon wire, psi
Control	150	120	145
Cudd cement	420	490	160

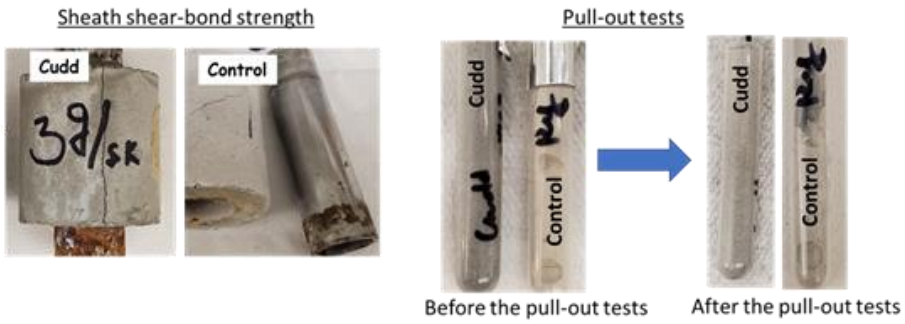

Figure 3: Appearance of Cudd and control cement after the sheath shear bond strength and before and after the pull-out tests.

3.3 Formulation Optimized for Electrical Resistivity

Although Cudd cement performance in all evaluations of mechanical properties and its rheological parameters was well-suited for filling small gaps that would be present in monitoring wells, the cement failed in developing electrical resistivity. The resistivity of the Cudd cement samples prepared with the Cudd Energy chemicals was 7 Ohm-m after 20 days of curing. Although it increased with time, there was no doubt that it was not going to reach the target values of more than 1000 Ohm-m.

To evaluate effect of the cement-modifying additives on electrical resistivity a series of samples was prepared based on the original design and tested for their resistivity using a modified ASTM C1760 method. The measurements were normalized to the resistivity of the original design, which was taken as 1 (Figure 4). The tested additives included gypsum, latex, micro glass fibers (MGF), various polymers and dispersants (dispersant 1 is LS, dispersant 2 was provided by Cudd), antifoam agent, calcium chelator (EDTA), microglass fibers (MGF), fly ash cenospheres (FCS), and FAF. Additionally, Cudd cement was tested without calcium chloride that originally was used as a set accelerator. The results of the resistivity measurements normalized to the control are shown in Figure 5. The green bars show designs with the resistivity above that of the control, blue bars with the resistivity like that of the control, yellow bars show designs with the resistivity slightly below that of the control, and the red bars refer to the designs with very low resistivity.

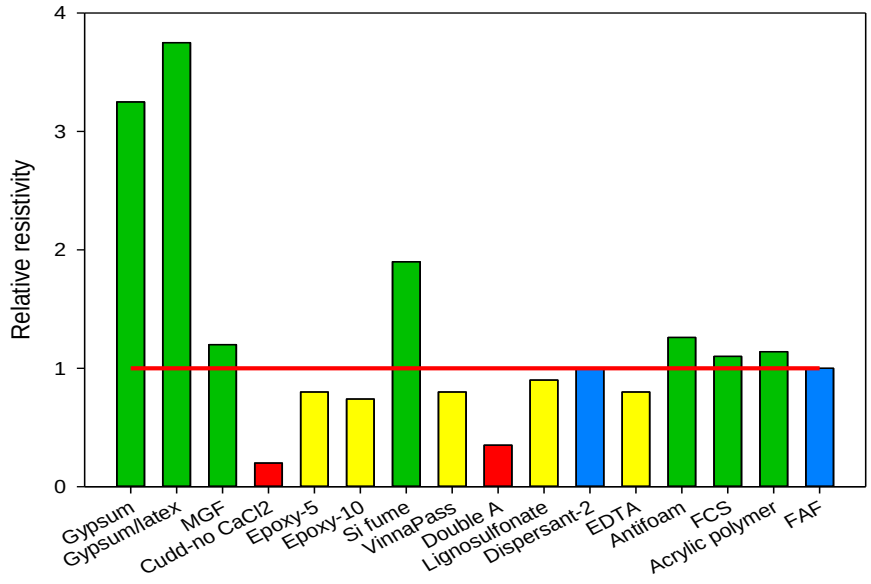

Figure 4: Relative resistivity of various cement designs measured with the 2-electrode method.

The following conclusions were drawn from these measurements. Increase of the cement content drastically decreased the resistivity ("double A" in the figure corresponds to 20% cement (class A), 50% slag, 30% pumice). Not surprisingly the Cudd cement with 59% bwob class A cement showed very low resistivity even without calcium chloride set accelerator. The resistivity of the control cement with 0.1% bwob antifoaming agent ("antifoam"), 10% bwob microglass fibers ("MGF"), and fly ash cenospheres ("FCS") that replaced pumice was slightly above that of the control. Silica fume almost doubled resistivity when it replaced 10% of pumice. Addition of gypsum strongly increased resistivity of the cement. The tested design with 5% bwob gypsum had resistivity three times above that of the control. The polymers showed mixed effect on the resistivity. Latex further increased resistivity of the sample with gypsum. Acrylic polymer slightly increased resistivity of the control, while epoxy-based polymer tested at 5% and 10% ("Epoxy-5" and "Epoxy-10") decreased resistivity of the cement as did 2% bwob vinyl acetate-based polymer ("VinnaPass"). Dispersants added at 0.2% bwob

showed mild effect on the resistivity. The resistivity of the slurry with the LS dispersant was below that of the control, the resistivity of the slurry with the Cudd dispersant ("dispersant-2") was like that of the control. The chelator added at 0.2% bwob decreased the resistivity. Finally, replacing pumice with FAF did not change the resistivity.

The results of the 2-electrode resistivity measurements were validated by the 4-electrode method that allows to eliminate contribution of the contact resistivity (Figure 5). The resistivity of the samples was measured after 20 days of hydration at room temperature; the measurements were performed twice on each sample.

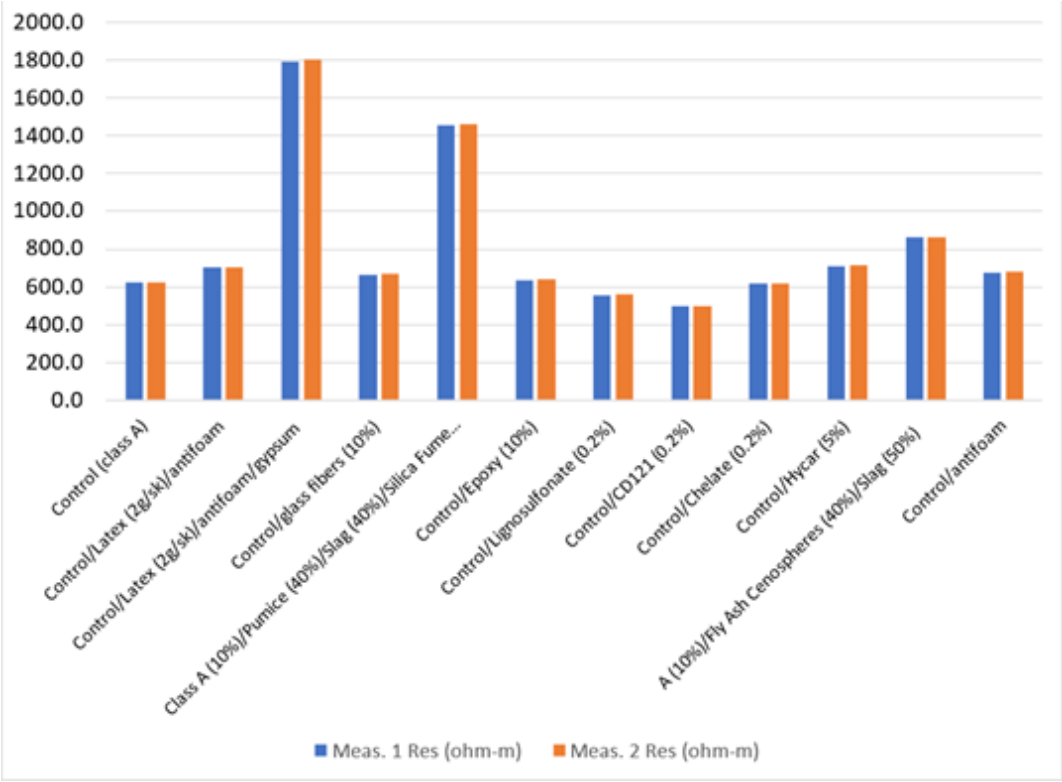

Figure 5: Resistivity of various cement designs measured with the 4-electrode method.

The results of the 4-electrode method for the most part agreed with those of the 2-electrode method. Gypsum and silica fume increased resistivity of the tested cement designs; the antifoam did not change it significantly. The effect of polymers on the resistivity was limited. Dispersants decreased it while fly ash cenospheres increased the resistivity of the cement. Some high resistivities were achieved after only 20 days of hydration. The cement design was further optimized for formulations to meet all the criteria including low rheological parameters of the slurry and development of mechanical properties. The resistivities of the tested formulations are given in Table 6 and their mechanical properties in Table 7. Selected formulations were further tested using API standard B-10 procedures to design field applicable formulations.

Table 6: Resistivity of cement formulations measured with 4-electrode method.

#	Curing time, days	Resistivity, Ohm-m	Formulation (latex at 3 gal/sk in all formulations)
1	26	2300	Cement (20%)/SF (15%)/Slag (25%)/FAF (40%)/Gypsum (10% bwob)/ latex
2	26	930	Cement (40%)/SF (20%)/FAF (40%)/Gypsum (15%)/ latex
3	26	1700	Cement (20%)/SF (15 wt.%)/FAF (40%)/Slag (30%)/Gypsum (5%)/ latex
4	26	360	Cement (40%)/SF (10%)/FAF (30%)/Slag (20%)/Gypsum (5%)/ latex
5	26	2070	Cement (10%)/SF (10%)/FAF (40%)/Slag (40%)/Gypsum (5%)/ latex
6	26	790	Cement (30%)/SF (10%)/FAF (30%)/Slag (30%)/Gypsum (5%)/ latex
7	19	640	Cement (30%)/SF (20%)/FAF (50%)/ Gypsum (15%)/ latex
8	19	-	Cement (20%)/SF (20%)/FAF (60%)/ Gypsum (15%)/ latex
9	19	300	Cement (30%)/SF (15%)/FAF (55%)/ Gypsum (15%)/ latex
10	19	420	Cement (30%)/SF (15%)/FAF (55%)/ Gypsum (10%)/ latex
11	19	1090	Cement (30%)/SF (15%)/FAF (40%)/Slag (15%)/Gypsum (10%)/ latex

12	19	1400	Cement (30%)/SF (15%)/FAF (25%)/Slag (30%)/Gypsum (10%)/ latex

Table 7: Mechanical properties of formulations from Table 6.

Sample #	Compressive strength, psi	Toughness, Nmm/mm^3	Rapture bond strength measured with Teflon wire, psi
Ref.	920 ± 60	0.11 ± 0.01	145
1	1640 ± 110	0.46 ± 0.08	171 ± 14
2	1660 ± 70	0.34 ± 0.01	135 ± 9
3	2560 ± 70	0.5 ± 0.09	-
4	3300 ± 10	0.68 ± 0.14	-
5	1570 ± 80	0.26 ± 0.04	62 ± 33
6	3180 ± 120	0.75 ± 0.46	-
7	1200 ± 31	0.22 ± 0.06	125 ± 7
9	1230 ± 50	0.39 ± 0.23	136 ± 14
10	1520 ± 50	0.39 ± 0.1	-
11	1770 ± 55	0.23 ± 0.04	154 ± 26
12	2300 ± 310	0.45 ± 0.1	166 ± 7

3.4 Formulations Optimized for Field Applications Using API Standard B-10

Optimization of cement formulations 1, 3 and 12 using API procedures produced very fluid slurries with low rheological parameters, high stability, and strength development above 1,000 psi. However, to reach the high-fluidity slurries the amount of added water was significantly increased (from about 0.3-0.4 water-to-blend ratio in the laboratory tests to ~0.6-0.7 in the API tests). The major difference in the slurries was a different batch of slag that was purchased for the field job. All other chemicals were identical for the work performed in the lab and with the API procedures. As stated above water strongly increase conductivity of slurries. To compensate for this water increase additional slurry optimization work was done. The following parameters were considered during the optimization – slurry density, rheological parameters, gel strength, slurry stability, strength development, slurry pumpability (thickening time).

3.5 Microstructural Investigation of High Electrical Resistivity in Cements

The experimental laboratory work described above allowed achieving high resistivity in cement formulations despite the presence of ionic additives necessary for control of other slurry and set cement properties. Since there is little information available in literature on design of high-resistivity cements it was of interest to understand the role of the blend components in the performance of the selected cement formulations. The resistivity (or conductivity) of cement matrix depends on the presence of ionic species and continuous media for their transport. Both these factors were likely controlled in the optimized cement designs. The strongest effect on the resistivity of cement was observed upon addition of gypsum. To understand effect of gypsum on the hydration of each of the blend components slurries of OPC, class A cement with gypsum and slag with gypsum were prepared and analyzed.

Figure 6 shows XRD patterns of neat class A OPC, cement with 20% by weight of cement (bwoc) gypsum and slag with 20% by weight of slag (bwos) gypsum after 30 days of hydration at room temperature. All the slurries were mixed by hand with water-to-cement ratio of 0.5 for OPC slurries and 0.57 for the slag slurry to achieve similar slump. The XRD pattern of slag alone is not shown since the material was mostly amorphous. Several clear trends are visible from the XRD patterns. As could be expected, addition of gypsum strongly increases intensity of ettringite peaks. Since small amount of gypsum is always added to the clinker to form ettringite and to prevent flash set of cement, the higher gypsum content results in formation of more ettringite. However, in the case of slag this increase was dramatic. The pattern changed from an amorphous material to that with high-intensity ettringite peaks, non-reacted gypsum, enstatite, and possibly clinoenstatite (ICDD:04-021-7224, not shown), srebrodolskite (ICDD:04-016-3580, not shown).

Earlier work suggested ettringite formation in the blends of slag and gypsum[12,13] or slag-clinker-gypsum[11]. At 2-to-1 slag-to-clinker ratio and 10% gypsum in a blend (similar to design #1 in the current study) very low concentration of calcium ions (0.454 mmol/L) and high pH of 13.09 was reported. In the case of blends tested in this work high pH would promote reactions of fly ash while low calcium ions concentration would result in limited electrical current.

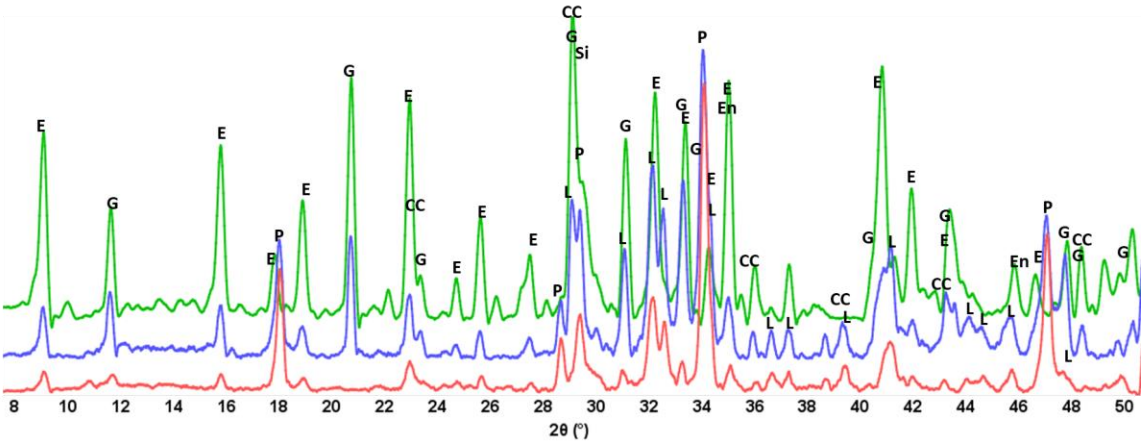

Figure 6: XRD patterns of neat cement (red), cement modified with 10% bwoc gypsum (blue) and slag modified with 10% bwos gypsum (green). E- ettringite (ICDD: 00-041-1451), G- gypsum (ICDD: 04-016-3025), CC- calcium carbonate (ICDD: 01-083-4608), L- larnite (ICDD: 00-033-0302), P- portlandite (ICDD: 00-044-1481), En- enstatite (ICDD: 00-019-0768), Si- silicon oxide (ICDD: 04-015-7167/04-007-2612).

Figure 7 shows changes in the crystalline composition of the original blend with the addition of silica fume, gypsum, and latex. Addition of gypsum to the blend results in crystallization of ettringite, which is evident from its high intensity peaks. Magnesium (calcium, iron) silicates form from alkali activated slag and fly ash. In the case of silica fume the peaks' intensities noticeably decrease suggesting decreased crystallinity of the matrix. Formation of larger amounts of C-S-H gel through reactions of silica fume with calcium ions is likely.

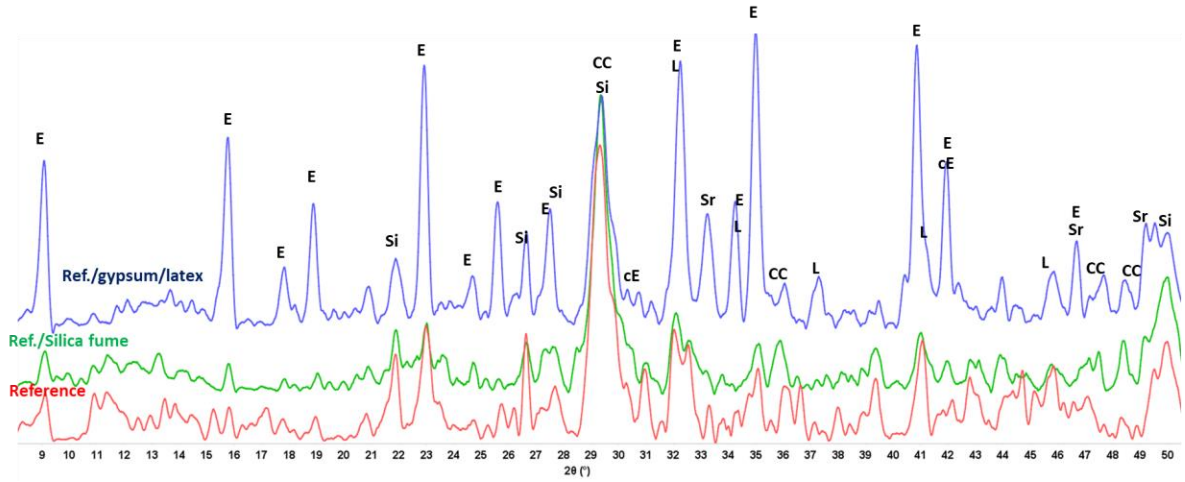

Figure 7: XRD patterns of the originally used cementing blend (reference) alone (red), with 15% silica fume, and with 10% gypsum and 3 gal/sk latex (blue) (percentage is by weight of blend). E- ettringite (ICDD: 00-041-1451), G- gypsum (ICDD: 04-016-3025), CC- calcium carbonate (ICDD: 01-083-4608), L- larnite (ICDD: 00-033-0302), P- portlandite (ICDD: 00-044-1481), En- enstatite (ICDD: 00-019-0768), cEn- clinoenstatite (ICDD: 04-021-7224), Sr – srebrodolskite (ICDD: 04-016-3580), Si- silicon oxide (ICDD: 04-015-7167/04-007-2612/01-073-6619).

Figures 8-11 show photomicrographs and elemental compositions of typical freshly broken samples of the reference design (Figure 8), and the reference design modified with gypsum (Figure 9), gypsum and latex (Figure 10), or silica fume (Figure 11). The reference sample was mostly amorphous with the features of about 10 microns in size, and the bigger ones being rich in silica (point 2). The Ca/Si ratio of the matrix itself was on the order of 1.4-2 with the denser parts being of lower calcium content (point 3).

Addition of gypsum visibly changed the sample's morphology (Figure 9). Long needles of ettringite crystals formed throughout the sample (point 1) incorporating calcium and water and leaving out silica to react with species released in alkali slag dissolution (Ca/Si in point 2 – 0.38, is noticeably lower than in the reference sample). Latex addition to the reference sample with gypsum (Figure 10) changes morphology of ettringite needles making them shorter and larger (point 1) while the matrix remains mostly amorphous with the larger adjacent hydration products being connected by elastic latex layer (image on the right) as was shown in the previous studies of latex-modified cement. The latex bridges and layers helped to enhance cement toughness and resistivity [5]. The matrix looks less dense than the matrix of the reference sample. This could be the result of delayed cement hydration in the presence of latex. Noticeable matrix

densification takes place with the addition of silica fume (Figure 11). As expected, the Ca/Si ratio decreases to below 1 value in the presence of silica fume. The images agree well with the XRD results showing formation of ettringite crystals in the presence of gypsum and mostly amorphous morphology of silica fume modified samples.

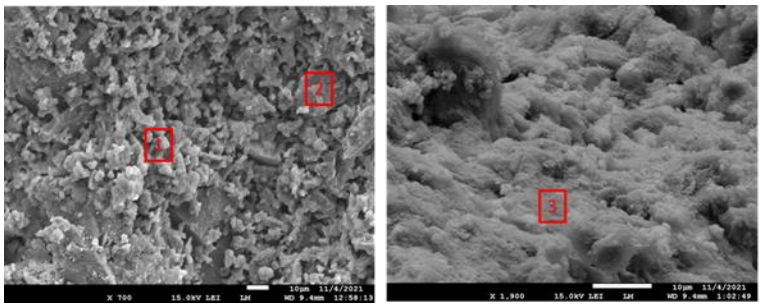

Point	1	2	3
O	79.82	80.08	90.18
Mg	1.51	1.06	0.69
Al	1.72	2.21	1.22
Si	5.48	11.48	3.14
S	0.25	-	0.20
K	0.63	1.47	0.13
Ca	10.59	3.70	4.44
Ca/Si	1.9	0.32	1.4

Figure 8: Photomicrographs of the reference sample after 30 days of hydration at room temperature and elemental composition in three different locations.

The hydration of calcium-aluminates in slag proceeds according to the following reactions [14,15]:

$3CaO \cdot Al_2O_3 + 6H_2O \rightarrow 3CaO \cdot Al_2O_3 \cdot 6H_2O$

In the presence of gypsum, the following reaction of ettringite formation takes place:

$3CaO \cdot Al_2O_3 \cdot 6H_2O + 26H_2O + 3CaSO_4 \rightarrow 3CaO \cdot Al_2O_3 \cdot 3CaSO_4 \cdot 32H_2O$

Ettringite formation consumes significant quantities of calcium and binds 32 water molecules. Calcium hydroxide released during the OPC hydration promotes slag reactions of silica and aluminum oxide dissolution that participate in ettringite and C-S-H gel development. It also interacts with the silica fume with formation of C-S-H gel. These interactions lead to decreased ionic concentrations in the pore solution, matrix densification, decreased pores connectivity, and, as a result increased resistivity of the cement. Silica fume further densifies the matrix and promotes reactions of calcium ions.

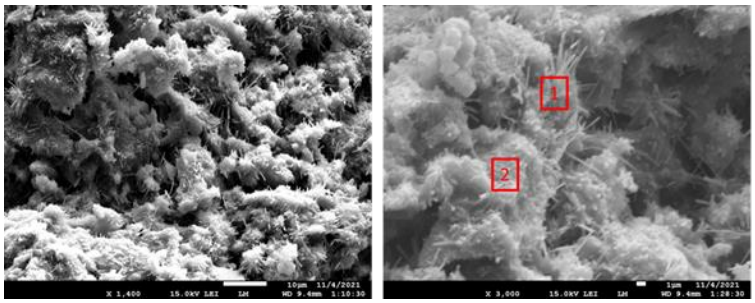

Point	1	2
O	48.69	47.03
Na	-	0.72
Mg	1.05	0.79
Al	5.13	5.53
Si	13.84	29.06
S	5.30	1.75
K	1.45	4.07
Ca	22.71	11.06
Fe	1.83	-

Figure 9: Photomicrographs of the reference sample with 10% bwob gypsum after 30 days of hydration at room temperature and elemental composition in two different locations.

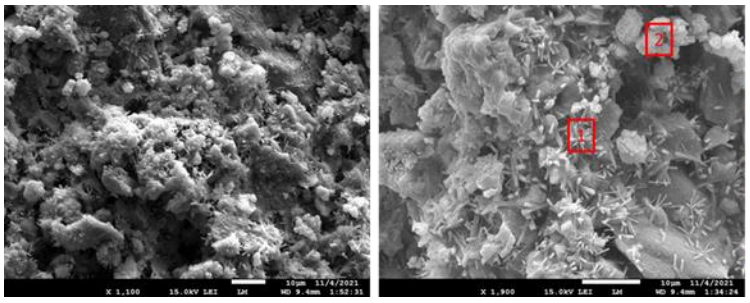

Point	1	2
O	40.37	39.17
Mg	4.77	3.85
Al	5.61	5.31
Si	14.70	18.29
S	5.74	3.18
K	1.04	1.28
Ca	27.77	28.93

Figure 10: Photomicrographs of the reference sample with 10% bwob gypsum and 3gal/sk latex after 30 days of hydration at room temperature and elemental composition in two different locations.

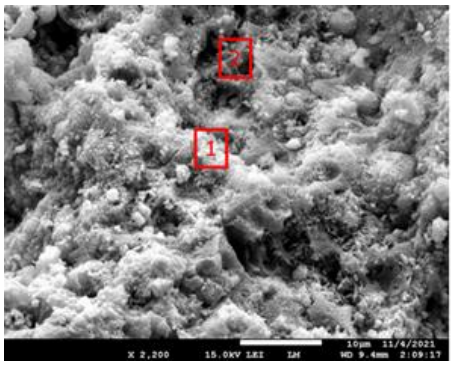

Point	1	2
C	-	61.96
O	52.57	21.29
Na	2.56	0.81
Al	18.36	6.44
Si	13.11	4.75
S	-	0.43
K	1.36	0.45
Ca	8.98	2.27
Fe	3.06	1.25

Figure 11: Photomicrographs of the reference sample with 15% bwob silica fume after 30 days of hydration at room temperature and elemental composition in two different locations.

4. CONCLUSIONS

Stable cement formulations with low rheological parameters, high toughness, improved bonding with metal and Teflon-covered wires, and high electrical resistivity were designed for cementing horizontal wells with monitoring equipment. The requirement of high electrical resistivity did not allow slurry modifications with common cementing additives, which are for the most part, ionic compounds strongly increasing conductivity of cement. A combination of latex and silica fume provided desirable rheological properties, including high slurry stability, low viscosity, and yield stress. Latex also provided more than 4 times improvement of cement toughness. A combination of slag, silica fume and gypsum allowed increase of electrical resistivity to above 2000 Ohm-m. An important role in this was attributed to the formation of ettringite molecules by slag and OPC in reactions with gypsum, which immobilized both calcium ions and water molecules transporting ionic species. Additionally, controlled slurry expansion improved bonding properties of the slurry. The drawback of high latex concentrations was a slow set at room temperature that could potentially be accelerated by the addition of non-ionic accelerators. Introduction of calcium chloride accelerator compromised resistivity of the cement even at low concentrations, so was abandoned. Nevertheless, the slurry remained stable even through the long setting time. Great variability of slag caused increased water requirement of the dry blend prepared for the field job. A second round of optimization was necessary to account for the water increase, which resulted in decreased resistivity. Slag variability is one of the major obstacles to slag applications for well cementing when several criteria must be met simultaneously.

5. ACKNOWLEDGMENTS

This publication was based on the work supported by the Geothermal Technologies Office in the US Department of Energy (DOE) Office of Energy Efficiency and Renewable Energy (EERE), under the auspices of the US DOE, Washington, DC, under contract No. DE-AC02-98CH 10886. Research was carried out in part at the Center for Functional Nanomaterials, Brookhaven National Laboratory, which is supported by the US Department of Energy, Office of Basic Energy Sciences, under Contract No. DE-SC0012704.

6. REFERECES

1. Yim, H. J., Bae, Y. H. & Jun, Y. Hydration and microstructural characterization of early-age cement paste with ultrasonic wave velocity and electrical resistivity measurements. *Construction and Building Materials* **303**, (2021).

2. Luo, T. & Wang, Q. Effects of graphite on electrically conductive cementitious composite properties: A review. *Materials* **14**, (2021).

3. Du, M., Jing, H., Gao, Y., Su, H. & Fang, H. Carbon nanomaterials enhanced cement-based composites: Advances and challenges. *Nanotechnol. Rev.* **9**, 115–135 (2020).

4. Shi, T., Li, Z., Guo, J., Gong, H. & Gu, C. Research progress on CNTs/CNFs-modified cement-based composites- A review. *Constr. Build. Mater.* **202**, 290–307 (2019).

5. Wei, J., Cheng, F. & Yuan, H. Electrical resistance and microstructure of latex modified carbon fiber reinforced cement composites. *J. Wuhan Univ. Technol. Mater. Sci. Ed.* **27**, 746–749 (2012).

6. Andrade, C., D'Andrea, R. & Rebolledo, N. Chloride ion penetration in concrete: The reaction factor in the electrical resistivity model. *Cement and Concrete Composites* **47**, 41–46 (2014).

7. Tian, Z., Li, Y., Zheng, J. & Wang, S. A state-of-the-art on self-sensing concrete_ Materials, fabrication and properties.pdf. *Compos. Part B* **177**, 107437 (2019).

8. Topu, I. B., Uygunolu, T. & Hocaolu, I. Electrical conductivity of setting cement paste with different mineral admixtures. *Construction and Building Materials* **28**, 414–420 (2012).

9. Tinnea, R., Tinnea, J. & Kuder, K. High-Early-Strength, High-Resistivity Concrete for Direct-Current Light Rail. *J. Mater.*

Civ. Eng. **29**, 04016260 (2017).

10. Tamas, F. D., Farkas, E., Voros, M. & Roy, D. M. Low-frequency electrical conductivity of cement, clinker and clinker mineral pastes. *Cem. Concr. Res.* **17**, 340–348 (1987).

11. Sun, H., Qian, J., Yang, Y., Fan, C. & Yue, Y. Optimization of gypsum and slag contents in blended cement containing slag. *Cem. Concr. Compos.* **112**, 103674 (2020).

12. Nguyen, H. *et al.* Byproduct-based ettringite binder " A synergy between ladle slag and gypsum". *Constr. Build. Mater.* **197**, 143–151 (2019).

13. Kim, J.-M., Choi, S.-M. & Han, D. Improving the mechanical properties of rapid air cooled ladle furnace slag powder by gypsum. *Constr. Build. Mater.* **127**, 93–101 (2016).

14. Liu, Z. *et al.* The mechanism of hydration reaction of granulated blast furnace slag-steel slag-refining slag-desulfurization gypsum-based clinker-free cementitious materials. *J. Build. Eng.* **44**, 103289 (2021).

15. Uchikawa, H. & Uchida, S. THE HYDRATION OF 11CaO. 7Al203. CaF 2 AT 20°C. *Cem. Concr. Res.* **2**, 681–695 (1972).